A Miniature GPS Receiver for Precise Orbit Determination of the Sunsat 2004 Micro-Satellite

Oliver Montenbruck
Deutsches Zentrum für Luft- und Raumfahrt (DLR), German Space Operations Center (GSOC), Wessling, Germany
Ben Nortier
Stellenbosch University (SU), Electronic Systems Laboratory, Stellenbosch, South Africa
Sias Mostert
Sun Space and Information Systems (Pty) Ltd (SunSpace), Stellenbosch, South Africa

BIOGRAPHY

Oliver Montenbruck is head of the GPS Technology and Navigation Group at DLR's German Space Operations Center (GSOC). He received his Ph.D. from Munich's University of Technology in 1991. Since 1987 he's been working as a flight dynamics engineer with focus on satellite orbit determination. His current field of work comprises the development of on-board navigation systems, spaceborne GPS applications, and satellite formation flying. He has written various text books on computational astronomy and satellite orbits as well as numerous papers on related topics.

Ben Nortier has completed his masters studies at the Electronic Systems Laboratory (ESL) of Stellenbosch University (SU). His thesis research focused on the space adaptation of an industrial GPS receiver that will be flown on the South African Sunsat 2004 satellite.

Sias Mostert is a full professor of electrical engineering at Stellenbosch University (SU) and director of Sun Space and Information Systems Ltd, a small company dedicated to the commercialization of SU space activities.

ABSTRACT

This paper describes the design of a miniature receiver for spaceborne GPS navigation and its use for precise orbit determination within the Sunsat 2004 project. Sunsat 2004 is the second remote sensing micro-satellite built by Stellenbosch University, South Africa. It carries a multi-spectral imaging payload with a resolution of 5 m and will be ready for launch in the second half of 2005. As part of the Sunsat 2004 mission, a Phoenix GPS receiver will provide navigation and timing information for real-time spacecraft operation. It is based on commercial-off-the-shelf hardware (SigTec MG5001) but employs software specifically designed for high-dynamics applications. The receiver offers L1 C/A code and carrier tracking on 12 channels with representative accuracies of 0.4 m and 0.7 mm. The real-time navigation solution provided by the Phoenix receiver is typically limited to an accuracy of about 5-10 m by broadcast ephemeris and ionospheric errors. Raw measurements will therefore be down-linked and processed offline for precise orbit determination. Here, ionospheric path delays can be fully eliminated using a linear combination of L1 code and carrier data. In combination with precise orbit and clock products of the International GPS Service (IGS), a 3D accuracy of 0.5m can thus be achieved. The receiver has extensively been validated in a GPS signal simulator testbed, and the resulting measurements are used to demonstrate the envisaged performance of the Sunsat 2004 orbit determination concept.

INTRODUCTION

Following the successful launch and operation of the Sunsat spacecraft in 1999-2001, Stellenbosch University (SU) is presently building its second remote sensing micro-satellite. Planned to be launched in late 2005, Sunsat 2004 will be smaller than 45 x 45 x 60 cm. It will be equipped with an optical telescope with a 1.5 m focal length and a multi-spectral sensor with a 5 m resolution. Its data will be used for agriculture, health (malaria) monitoring, disaster mitigation and infrastructure planning in South Africa.

Navigation information for spacecraft operations and geo-coding of the image data will be provided by a miniature GPS receiver that has jointly been developed by SU and the German Space Operations Center (DLR/GSOC). It builds up on DLR's Orion-S spaceborne GPS receiver but employs an advanced chipset, which allows a tighter integration of the receiver hardware and lower power consumption.

GPS navigation fixes and raw measurements will be recorded onboard and dumped during passes over the Stellenbosch or Antarctica ground station. While the navigation fixes are used for quick-look orbit determination, more refined orbits will be derived from the raw measurements in combination with precise GPS orbit and clock solutions of the International GPS Service (IGS). In this process, ionospheric errors can be eliminated by forming the GRAPHIC (Group and Phase Ionospheric Calibration) linear combination of single-frequency pseudorange and carrier phase measurements. Both a purely kinematic positioning and a dynamic orbit determination scheme are currently under consideration. Either of them is expected to deliver a 3-dimensional position restitution of better than 1m, which is compatible with the resolution of the best spaceborne imaging sensors presently employed on non-military spacecraft.

Following an introduction to the Sunsat mission, the paper provides a description of the receiver hard- and software and addresses the adopted approach for porting the GPS Orion software to the new system architecture. The tracking performance is documented based on signal simulator tests for a standard low Earth orbit scenario. Finally the SUNSAT orbit determination concept is described and results from hardware-in-the loop simulations are presented.

SUNSAT 2004

Sunsat 2004 is the second satellite built by Stellenbosch University (SU). Its predecessor, Sunsat, was successfully launched in 1999 and operated for two years. Sunsat carried a pushbroom imager with 15 m resolution, a BlackJack GPS receiver provided by NASA/JPL as well as an amateur radio communication unit. Sunsat 2004 will again serve as a remote sensing satellite but aims to achieve a higher ground resolution at lower total system cost [1].

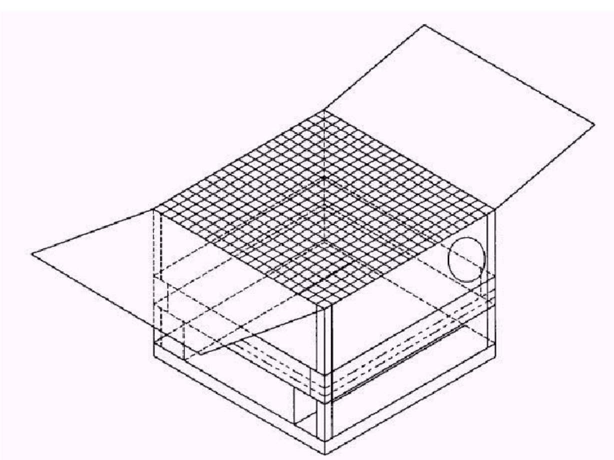

Fig. 1 Sunsat 2004 configuration

The total size of Sunsat 2004 will not exceed a dimension of 45 cm x 45 cm x 60 cm for maximum flexibility in the choice of available launchers (Fig. 1). Various options are presently examined and the spacecraft is targeted to be ready for launch in the second half of 2005. The basic spacecraft design makes use of the Sunsat heritage with mission specific adaptations. The satellite will be constructed from ‘building brick’ modules that can be configured in various geometric forms without redesigning the internals of the modules. All modules will be stacked in racks of 18 cm x 16 cm footage and interfaced via CAN bus. The spacecraft structure will be compatible with the Sunsat bottom tray, carrying further trays of the same size. A single solar panel, unfolded after separation from the launcher, will provide the required onboard power for bus and payload operation. A redundant S-band transmitter will be used for high-speed downlink of image data during contacts with the Stellenbosch and Antarctica groundstations. Telecommanding is performed via a UHF uplink.

The primary objective of the Sunsat 2004 mission consists in the collection of remote sensing data for agriculture, health (malaria) monitoring, disaster mitigation and infrastructure planning in South Africa. The spacecraft will therefore be equipped with an optical telescope of 1.5 m focal length and a multi-spectral sensor offering a 5 m resolution. In order to manage the high data-volume generated by these sensors and allow an efficient down-link in real-time, a combination of image processing and lossy image compression will be employed onboard the spacecraft [2]. A flash memory of 1-8 GByte size allows 20-150 square images at a 6000 pixel size to be stored and processed. Supplementary to the imaging payload, the use of a dual frequency GPS receiver (NovAtel OEM4-G2 or JPL BlackJack) for ionospheric occultation measurements is currently under investigation.

The Attitude Determination and Control System (ADCS) of Sunsat 2004 comprises a magnetometer and torque rods as well as reaction wheels and fiber optical gyros (FOG) for full three-axis control and accurate Sun/Earth pointing. Navigation data for ADCS support and time synchronization are provided by a single frequency GPS receiver (Phoenix). Since availability of the dual-frequency receiver science payload is presently not ensured, precise orbit determination (POD) must also be supported by single-frequency GPS. Raw code and carrier measurements of the Phoenix receiver will therefore be included into the telemetry data stream. Using the ionosphere free GRAPHIC linear combination, an accuracy of up to 0.5 m is envisaged for the single-frequency POD, which is well compatible with the resolution of the Sunsat 2004 imaging system.

THE PHOENIX GPS RECEIVER

The Phoenix receiver selected for use on Sunsat 2004 is a follow-on of DLR's flight proven Orion-S/HD [3,4] receivers for space and high-dynamics applications. Like the Orion, it combines commercial-off-the-shelf (COTS) hardware components with a GPS signal processing software specifically designed for navigation of low Earth orbit satellites and sounding rockets.

The receiver is built around the GP4020 chip of Zarlink, which combines a 12 channel correlator for L1 C/A code and carrier tracking, a microcontroller core with 32 bit ARM7TDMI microprocessor and several peripheral functions (real-time clock, watchdog, 2 UARTS etc.) in a single package. This offers a high level of compatibility with the GP2021 correlator and ARM60P microprocessor employed within the GPS Orion receiver and thus provides a cost-effective choice for advancing to more miniaturized space receivers.

Fig. 2 Phoenix (MG5001) receiver board

Presently, two manufacturers (Sigtec and CMC/NovAtel) have employ the GP4020 chip in commercial receiver boards (MG5001, Superstar II) for terrestrial mass market applications. In view of good experience with the Orion-S receiver that is likewise based entirely on COTS technology, it was decided to avoid independent hardware developments and modify the MG5001 OEM receiver (Fig. 2) to run the Orion-S spaceborne receiver software. The companion Sigtec MG5021 Development Kit was used for software development and debugging.

The MG5001 board provides a 512 kByte flash EPROM for storing the receiver software and a 256 kByte RAM memory for run-time code and data. If desired, the RAM can be doubled for large applications extending the standard receiver functionality. Supplementary to the external memory modules, the GP4020 chip provides a fast internal RAM of 32 kByte size. It is battery buffered and serves as non-volatile memory for critical receiver parameters almanac, broadcast ephemerides and orbit elements of the user spacecraft.

The backup battery also drives a 32.768 kHz clock crystal and a real-time clock (RTC) inside the GP4020 to maintain the current time during deactivation of the main power supply. By default, the MG5001 receiver is operated at a +5V supply voltage, which is internally converted to the 3.3V required by the correlator and microprocessor.

UARTs integrated into the GP4020 chip offer two serial ports for communication, but supplementary line drivers are required to achieve RS232 or RS422 compatible signal levels. In combination with a small boot routine residing in the GP4020's internal boot EPROM, the primary communication port can also be used for "on-the-fly" uploads of new receiver software.

The shielded RF frontend employs a GP2015 chip to down convert and filter the L1 signal and perform a 2 bit digitization. Narrow band filtering of the intermediate frequency is provided by Murata saw filter. Other than the Orion receiver, the Phoenix (MG5001) receiver provides two cascaded low noise amplifiers, which notably reduce the required antenna gain. Depending on the particular antenna configuration, carrier-to-noise ratio improvements of up to 3 dB-Hz have been observed with the Phoenix receiver compared to its predecessor.

Despite a high communality of the correlators and microprocessors, the Orion receiver software could not be employed as is for the Phoenix receiver due to subtle differences in peripheral functions (e.g. UART design and interrupt control) and the ARM development systems. Originally, it was therefore decided to retain the µITRON operating system of SigTec's proprietary MG5001 software and merge it with the signal tracking and navigation functions of the Orion-S firmware. Based on experience gained in [5], the port was readily completed but suffered from occasional instabilities attributed to interrupt control problems. Also, use of the µITRON real-time operating system resulted in a notable increased size of the executable code without providing relevant benefits. A full port of the GPS Orion operating system including tasking, interrupt control and UART handling was therefore conducted at last, which resulted in lean and highly stable receiver software.

As mentioned above, the receiver is specifically designed to work under specific signal conditions of satellite and sounding rocket applications. It uses a wide-band 3rd order phase-locked loop with FLL assist for carrier tracking and a narrow-band carrier aided delay-lock loop for code tracking. This ensures robust tracking and avoids systematic steady state errors even under high signal dynamics. All measurements are synchronized to integer GPS seconds with a representative accuracy of 0.2µs and a 1 pulse-per-second hardware signal is generated at the same instant. If required, intermitted operation of the receiver is supported through orbital elements stored in non-volatile memory, the battery backed-up real-time clock and an orbit propagator. These allow a warm or hot start with typical times to first fix of 2 min and 30 s respectively [6].

The Phoenix receiver provides raw pseudorange, carrier phase and Doppler measurements with noise levels of 0.3 m, 0.5 mm and 0.06 m/s at a carrier-to-noise ratio of 45 db-Hz (Fig. 3). Furthermore, it offers carrier phase smoothed pseudoranges (ca. 6 cm/s noise level) and carrier based range-rate measurements (accurate to 1-2 cm/s). In contrast to other receivers based on the GP2021 or GP4020 correlator, carrier phase measurements obtained with DLR's Phoenix/Orion software exhibit integer differences in double difference measurements, thus supporting relative navigation and attitude determination applications using multiple receiver units.

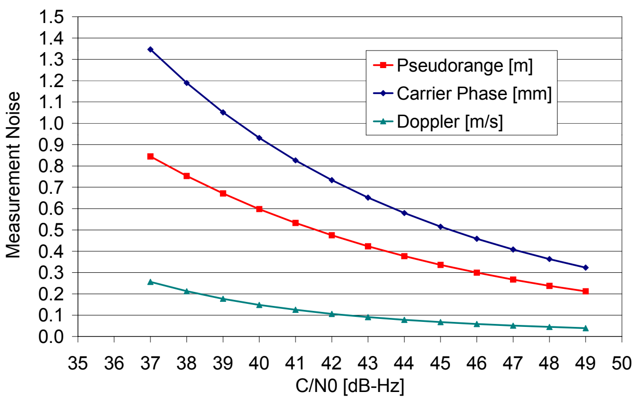

Fig. 3 Code and carrier noise of Phoenix receiver from zero-baseline signal simulator test for a low Earth orbit scenario

Compared to its predecessor, the Phoenix receiver features a notably lower power consumption (ca. 0.7 W) as well as a smaller form factor (70 x 47 x 11 mm). It can thus be used on a wide range of nano- and micro-satellites with restricted onboard resources. Tests conducted with a Co-60 gamma radiation source [7] demonstrate that the MG5001 receiver board can tolerate a total ionizing dose (TID) of up to 15 krad (Si). This is compatible with previous tests [8] and flight experience for the GP2021 chipset and is expected to allow operation in low Earth orbit (LEO) for at least several years.

SUNSAT ORBIT DETERMINATION

Following the deactivation of Selected Availability (S/A), the orbit determination accuracy of LEO satellites using single frequency GPS is mainly limited by broadcast ephemeris errors and ionospheric path delays. Out of these, broadcast ephemeris errors are only relevant for real-time applications and exhibit a representative standard deviation of about 4 m [9]. Ionospheric range errors, in contrast, at low elevations may amount to 10-20 m [10] and dominate the error budget of post-processed single-frequency GPS solutions. Even spacecraft orbiting the Earth above the electron density maximum may be notably affected by ionospheric errors. As an example, the single-frequency navigation solution for the Proba satellite was found to exhibit a 3D rms error of 6.5 m and a systematic radial offset of about 3 m [11] despite and altitude of 650 km.

As proposed by Yunck [12] the problem of ionospheric path delay in single frequency GPS positioning can be overcome by using a specific linear combination of code and carrier phase measurements. It makes use of the fact that carrier phases exhibit a phase change in dispersive media that is equal in size to the code delay I, but opposite in sign. Denoting the range between the GPS satellite and the receiver by ρ, the GPS and receiver clock offsets by cdt_{GPS} and cdt, and the carrier phase bias by B, the code and carrier measurements can thus be expressed as

$$\begin{aligned} \rho^{\mathrm{C/A}} &= \rho + c(\delta t - \delta t_{\mathrm{GPS}}) + I \\ \rho^{\mathrm{L1}} = \lambda\varphi &= \rho + c(\delta t - \delta t_{\mathrm{GPS}}) - I - B \ . \end{aligned} \quad (1)$$

Evidently the ionospheric range delay can be eliminated by forming the arithmetic mean

$$\begin{aligned} \rho^* &= (\rho^{\mathrm{C/A}} + \rho^{\mathrm{L1}})/2 \\ &= \rho + c(\delta t - \delta t_{\mathrm{GPS}}) - B/2 \ , \end{aligned} \quad (2)$$

which is also known as GRAPHIC (Group and Phase Ionospheric Calibration) measurement [12]. Other than the ionosphere free linear combination of dual frequency P(Y)-code measurements (which exhibits roughly three times the single frequency code noise), the GRAPHIC measurements exhibit a noise level that is roughly one half of the C/A code noise (i.e. ca. 0.2 m for the Phoenix receiver). However, the benefits of GRAPHIC observations come at the expense of a measurement bias that is different for each channel and inhibits their direct use for single point positioning.

The GRAPHIC bias $b=B/2$ originates from the carrier phase bias and is therefore constant during intervals of continued carrier phase tracking. This fact can be used to perform a global (non-linear) least-squares adjustment of epoch-wise receiver positions and clock-offsets

$$\boldsymbol{X} = (\boldsymbol{x}_1; \ldots; \boldsymbol{x}_J) \quad \text{with} \quad \boldsymbol{x}_j = (r_j; c\delta t_j) \quad (3)$$

as well as pass-by-pass biases

$$\boldsymbol{B} = (b_1; \ldots; b_M) \quad (4)$$

from GRAPHIC observations

$$\boldsymbol{z} = (\rho_1^*; \ldots; \rho_K^*) \quad (5)$$

collected over extended data arcs. Assuming a 30 s data interval, the vector of unknowns comprises a total of 480 position and clock components per one hour data arc. In case of LEO satellites the GPS visibility varies rapidly and about two to three GRAPHIC biases have to be adjusted per active tracking channel in the same time frame.

Even so the number of observations (ca. 1000/h) well exceeds the total number of estimation parameters (ca. 500/h) in this case, the normal equations turn out to be singular due to the simultaneous estimation of clock offsets and bias parameters [13]. A priori constraints

$$\begin{aligned} \mathrm{E}(\boldsymbol{B}) &= \boldsymbol{B}_{\mathrm{ap}} \\ \mathrm{E}[(\boldsymbol{B}-\boldsymbol{B}_{\mathrm{ap}})(\boldsymbol{B}-\boldsymbol{B}_{\mathrm{ap}})^T] &= \sigma_{B,\mathrm{ap}} \cdot \boldsymbol{1} \end{aligned} \tag{6}$$

for the biases must therefore be incorporated into the normal equations to enable a proper solution of the least-squares problem. Given the typical size of ionospheric path delays, it is generally appropriate to obtain the a priori bias values from the average difference of code and carrier measurements over a given pass:

$$b_{m,\mathrm{ap}} = \frac{1}{2}\overline{\left(\rho^{\mathrm{C/A}} - \rho^{\mathrm{L1}}\right)}_{m,E>30°} \tag{7}$$

For best results, only high elevation observations (e.g. elevation E>30°) are included into this average, and an a priori variance of

$$\sigma_{B,\mathrm{ap}} = 100\ \mathrm{m} \tag{8}$$

is adopted.

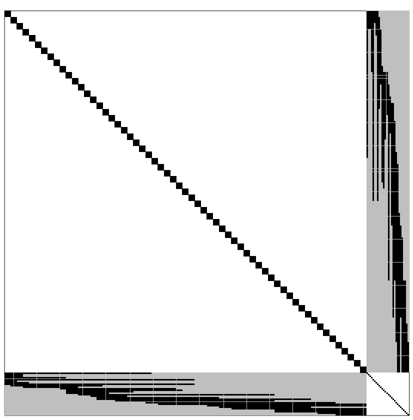

Fig. 4 Block structure of the normal equations matrix for the adjustment of position/clock and bias parameters from GRAPHIC observations [13].

Due the large number of estimation parameters involved in the global adjustment of position/clock ($\boldsymbol{X}$) and bias ($\boldsymbol{B}$) values, a direct solution of the resulting normal equations

$$\begin{pmatrix} \boldsymbol{N}_{XX} & \boldsymbol{N}_{XB} \\ \boldsymbol{N}_{BX} & \boldsymbol{N}_{BB} \end{pmatrix} \begin{pmatrix} \Delta\boldsymbol{X} \\ \Delta\boldsymbol{B} \end{pmatrix} = \begin{pmatrix} \boldsymbol{n}_X \\ \boldsymbol{n}_B \end{pmatrix} \tag{9}$$

for the corrections $\Delta\boldsymbol{X}$ and ΔB is generally impractical. Instead, a block elimination technique is employed based on the fact that the largest matrix $\boldsymbol{N}_{XX}$ is made up of J submatrices of dimension 4x4 placed along the main diagonal. This allows an easy computation of its inverse and a pre-elimination of the unknowns $\Delta\boldsymbol{X}$. Thus corrections of the a priori bias values can be computed from the relation

$$\Delta\boldsymbol{B} = \left(\boldsymbol{N}_{BB} - \boldsymbol{N}_{BX}\boldsymbol{N}_{XX}^{-1}\boldsymbol{N}_{XB}\right)^{-1}\left(\boldsymbol{n}_B - \boldsymbol{N}_{BX}\boldsymbol{N}_{XX}^{-1}\boldsymbol{n}_X\right) \tag{10}$$

Thereafter, corrections of the a priori position and clock states are obtained from the relation

$$\Delta\boldsymbol{X} = \boldsymbol{N}_{XX}^{-1}\left(\boldsymbol{n}_X - \boldsymbol{N}_{XB}\Delta\boldsymbol{B}\right) \tag{11}$$

[13]. Since a priori position and clock solutions obtained from a traditional single point positioning are already accurate to about 10 m, a single iteration is generally sufficient to obtain highly accurate navigation solutions from the global adjustment of GRAPHIC measurements.

The purely kinematic positioning scheme described above, can readily be extended to allow a dynamic orbit determination of LEO satellites from GRAPHIC data. using. In accord with the targeted accuracy of 0.5-1 m, a dynamical model accounting for the aspherical gravitational field of the Earth, air drag, point mass perturbations of the Sun and Moon, solar radiation pressure as well as solid Earth tides is employed [14]. In additions empirical accelerations in the radial, along-track, cross-track direction are considered to account for residual imperfections of the deterministic force model. The equation of motion and the (simplified) variational equations are numerically integrated using a variable-order variable stepsize multistep method, which ensures both computational efficiency and accurate results.

The predicted trajectory is fully described by the epoch state vector $\boldsymbol{y}_0$ and a total of five force model parameters

$$\boldsymbol{p} = (C_{\mathrm{R}}, C_{\mathrm{D}}, a_{\mathrm{R}}, a_{\mathrm{T}}, a_{\mathrm{N}}) \quad , \tag{12}$$

namely the radiation pressure coefficient (C_{R}), the drag coefficient (C_{D}) an d the three empirical accelerations (a_{R}, a_{T}, a_{N}). These are combined into an eleven-dimensional vector

$$\boldsymbol{Y} = (\boldsymbol{y}_0, \boldsymbol{p}) \tag{13}$$

that replaces the epoch-wise positions $\boldsymbol{r}_{\mathrm{j}}$ in the least squares estimation. On the other hand, the receiver clock offsets

$$\boldsymbol{T} = (c\delta t_1; \ldots; c\delta t_J) \quad , \tag{14}$$

cannot adequately be described by a dynamical model and still need to be adjusted on an epoch-by-epoch base.

As part of the orbit determination the clock offsets $\boldsymbol{T}$, the state and force model parameters $\boldsymbol{Y}$, and the biases $\boldsymbol{B}$ need to be adjusted in an iterated least-squares estimation process. In analogy with the kinematic processing, the resulting normal equations may again be partitioned into a form

$$\begin{pmatrix} \boldsymbol{N}_{T,T} & \boldsymbol{N}_{T,YB} \\ \boldsymbol{N}_{YB,T} & \boldsymbol{N}_{YB,YB} \end{pmatrix} \begin{pmatrix} \Delta\boldsymbol{T} \\ \Delta\boldsymbol{YB} \end{pmatrix} = \begin{pmatrix} \boldsymbol{n}_T \\ \boldsymbol{n}_{YB} \end{pmatrix} \tag{15}$$

suitable for pre-elimination of the clock offset parameters (cf. Fig. 4). Corrections to the a priori parameters are then obtained from the expression

$$\Delta \boldsymbol{YB} = \left(\boldsymbol{N}_{YB,YB} - \boldsymbol{N}_{YB,T}\boldsymbol{N}_{T,T}^{-1}\boldsymbol{N}_{T,YB}\right)^{-1} \times \left(\boldsymbol{n}_{YB} - \boldsymbol{N}_{YB,T}\boldsymbol{N}_{T,T}^{-1}\boldsymbol{n}_{T}\right). \quad (16)$$

Depending on the quality of the initial values of the estimation parameters, multiple iterations (3-5) are generally required to achieve a fully converged solution. Other than the kinematic processing, however, the dynamical orbit determination scheme can also handle epochs with less than four observed GPS satellites and is able to generate continuous trajectory information for geocoding and photogrammetric image processing.

SIMULATIONS

To assess the tracking and orbit determination accuracy achievable within the Sunsat 2004 project, various hardware-in-the-loop tests have been conducted. GPS signals for a LEO satellite scenario were generated with a Spirent STR4760 12 channel GPS signal simulator. Without loss of generality, a near circular, near polar orbit at a 450 km altitude has been assumed in the simulation (cf. [15]). A constant ionospheric electron content of 20 TECU was, furthermore, assumed, which results in a vertical path delay of about 3.2 m.

A Phoenix receiver was connected to the signal simulator via a preamplifier and the signal strength was adjusted to obtain carrier-to-noise ratios representative of an active antenna in terrestrial applications. Navigation solutions were generated in real-time and raw measurements were recorded for data analysis and offline orbit determination. GRAPHIC measurements were then formed from code and carrier measurements collected during a two hours simulation at a 10 s sampling rate.

Due to lacking information on the simulator internal trajectory model, a dynamical orbit determination turned out to be non-feasible when aiming at a sub-meter level accuracy. Only kinematic solutions could therefore be computed based on the global adjustment described above. In total some 2100 position components, 700 clock offsets and 50 GRAPHIC biases had to be adjusted for the simulated 2h data arc. The solution of the associated normal equations required less than half a minute on a 600 MHz Pentium processor.

As shown in Fig. 5, the resulting position solutions exhibit errors of about 40 cm, 25 cm, and 17 cm, respectively, in radial, along-track, and cross-track direction, which are consistent with the accuracy (ca. 20 cm) of the Phoenix GRAPHIC measurements.

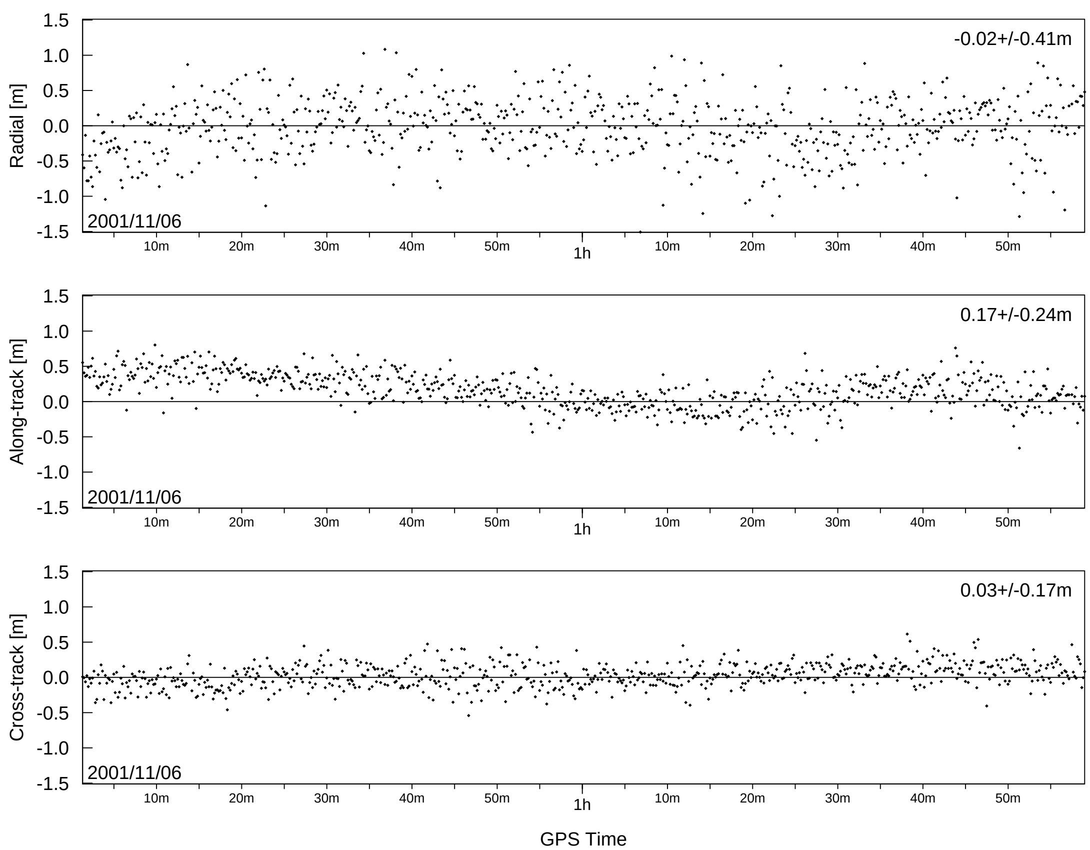

Fig. 5 Residuals of kinematic position solution from Phoenix GRAPHIC measurements for a simulated LEO arc of 2h duration

SUMMARY AND CONCLUSIONS

A 12-channel single-frequency GPS for the upcoming Sunsat 2004 mission has been presented. The Phoenix receiver is based on SigTec's commercial MG5001 board but employs a signal processing software specifically adapted for space applications. To fully benefit from the excellent tracking accuracy of the Phoenix receiver, a special processing of the raw measurements is proposed that is able to eliminate ionospheric effects through a linear combination of C/A code and L1 carrier phase measurements. Hardware-in-the-loop simulations have been conducted to verify the proper function of the receiver and the navigation concept. The overall 3D rms position error achieved in this way (53 cm) is well below one meter and fully satisfies the Sunsat 2004 mission requirements.

ACKNOWLEDGMENTS

The authors would like to thank Peter Mumford and Chris Rizos for valuable discussions and advice on the GP4020 adaptation of the GPS Orion software. Access to the STR4760 signal simulator was kindly provided by Kayser-Threde, Munich.

REFERENCES

[1] Milne, G.W., Mostert S., Steyn H.; *Sunsat 2004 – Progress and Status*; IAC-03-IAA.11.1.05; 54th International Astronautical Congress; 20 Sep. – 03 Oct. 2003, Bremen, Germany (2003).

[2] Mostert S., Kriegler E.; *Implementing and Image Processing System for the Next Generation Earth Observation Sensors for the Sunsat 2 Micro-Satellite Programme*; IAA-B4-0902; 4th IAA Symposium on Small Satellites for Earth Observation, April 7-11, 2003, Berlin (2003).

[3] Montenbruck O., Markgraf M., Leung S., Gill E.; *A GPS Receiver for Space Applications*; ION GPS 2001 Conference, Salt Lake City, 12-14 Sept. 2001 (2001).

[4] Montenbruck O., Markgraf M.; *User's Manual for the GPS Orion-S/-HD Receiver*; GTN-MAN-0110; Issue 1.0, DLR/GSOC (2003).

[5] Nortier B.; *A Spaceborne GPS Receiver*; Master's Thesis, University of Stellenbosch, South Africa (2003).

[6] Leung S., Montenbruck O., Bruninga R.; *GPS Tracking of Microsatellites - PCsat Flight Experience*; 5th International ESA Conference on Guidance, Navigation and Control Systems, 22-25 October 2002, Frascati, Italy (2002).

[7] Markgraf M., Montenbruck O.; *Total Ionizing Dose Testing of the Orion and Phoenix GPS Receivers*; DLR TN 04-01, Deutsches Zentrum für Luft- und Raumfahrt, Oberpfaffenhofen (2004).

[8] Unwin M.J., Oldfield M.K., Underwood C.I., Harboe-Sorensen R., *The use of commercial technology for spaceborne GPS receiver design*; ION-GPS-1998, Sep. 15–18, 1998, Nashville (1998).

[9] *GPS broadcast ephemeris accuracy statistics*; University of New Brunswick, Department of Geodesy and Geomatics Engineering; http://gge.unb.ca/gauss/htdocs/grads/orbit/; (2003/12/02).

[10] Montenbruck O., Gill E.; *Ionospheric Correction for GPS Tracking of LEO Satellites*; The Journal of Navigation 55, 293-304 (2002).

[11] Montenbruck O., Vuilleumier P.; *In-flight Performance Analysis of the PROBA Onboard Navigation System*; DLR-GSOC TN 03-02; Deutsches Zentrum für Luft- und Raumfahrt, Oberpfaffenhofen (2003).

[12] Yunck T.P.; *Orbit Determination*; in: Parkinson B.W., Spilker J.J. (eds.); *Global Positioning System: Theory and Applications*. AIAA Publications, Washington DC (1996).

[13] Montenbruck O.; *Kinematic GPS Positioning of LEO Satellites using Ionosphere-free Single Frequency Measurements*; Aerospace Science and Technology **7**, 396-405 (2003).

[14] Montenbruck O., Gill E.; *Satellite Orbits*; Springer Verlag, Heidelberg (2000).

[15] Montenbruck O., Holt G.; *Spaceborne GPS Receiver Performance Testing*; DLR-GSOC TN 02-04; Deutsches Zentrum für Luft- und Raumfahrt, Oberpfaffenhofen (2002).